Multiple magnetic states and metal-insulator transition in $Ca_{1-x}Na_xV_2O_4$ with double-chain structure

Hiroya Sakurai[*]

National Institute for Materials Science, Namiki 1-1, Tsukuba, Ibaraki 305-0044, Japan
(Received 6 February 2008; revised manuscript received 1 August 2008; published 10 September 2008)

Vanadium oxides with double-chain structures show various interesting physical properties, although the properties have not been systematically understood due to the lack of the investigation in a wide range of vanadium valence. In this paper, in order to establish a detailed magnetic and electrical phase diagram for $Ca_{1-x}Na_xV_2O_4$, the magnetic properties, electrical resistivity, and specific heat of this system were measured for various x values as a function of the temperature (T) and magnetic field (H). In the case of NaV_2O_4, a sharp antiferromagnetic (AF) transition was observed at $T_N = 140$ K as reported previously. T_N decreases to ~ 100 K with decreasing x down to $x_{c_1} \sim 0.78$, maintaining metallic conductivity. Three magnetic subphases were discovered depending on x, T, and H. On the other hand, below x_{c_1}, a broad peak in the magnetic susceptibility appears instead of the sharp peak due to the AF transition. The temperature corresponding to the maximum, T_{max}, rapidly increases up to ~ 340 K with decreasing x down to approximately 0.33 and then slightly decreases down to 300 K for CaV_2O_4, which is electrically insulating. For $x = 0.75$ and 0.67, metal-insulator transitions occurred at T_{max}. These complex phase relations, as well as the origin of the magnetism of this system, are discussed comparing it with other compounds.

I. INTRODUCTION

Vanadium oxides with the calcium-ferrite-type structure are expected to show very interesting physical properties due to their double-chain structural units, which can cause geometrical frustration and low-dimensional electron correlations (Fig. 1). Indeed, some vanadium hollandites, which are composed of similar double chains, although the way in which they are connected is different, exhibit metal-insulator transitions with interesting magnetic states.[1–4] In the case of the hollandites, the formal valence of the vanadium ion tends to be higher, closer to +4, as expected from the chemical formula of $A_xV_8O_{16}$ (A: alkaline metal, alkaline-earth metal and others, and $0 \leq x \leq 2$). On the other hand, the physical properties of double chains with a lower valence can be investigated by using calcium-ferrite-type vanadium oxides of AV_2O_4. However, only a few vanadium oxides, such as CaV_2O_4 and $Y_{0.5}V_2O_4$, adopt this kind of structure,[5,6] and very limited studies on the physical properties of these calcium-ferrite-type vanadium oxides have been performed thus far.

CaV_2O_4 is electrically insulating and shows a broad maximum in the temperature dependence of the magnetic susceptibility. Fukushima *et al.*[7] suggested possible gapless chiral ordering because no magnetic ordering was detected by their ^{51}V nuclear magnetic resonance (NMR) measurements and the spin-lattice relaxation rate $1/T_1$ was proportional to temperature, which implied anomalous spin dynamics. Recently, however, detailed NMR measurements by Zong *et al.*[8] revealed that CaV_2O_4 exhibits antiferromagnetic ordering at $T_N = 78$ K (in the case of powder). In the antiferromagnetic state, the local magnetic moments were found to be antiferromagnetically aligned in a chain with slight canting from the c direction of the *Pnma* setting. Older neutron-diffraction data also indicate magnetic ordering at 4.2 K.[9] At present, the origin of the contradiction between Fukushima *et al.* and the

others is still unclear. Sample dependence may need to be considered because the temperature corresponding to the broad maximum of the susceptibility, T_{max}, reported by the former was approximately 220 K while that reported by Zong *et al.* was $T_{max} = 280$ K. In addition, the T_N value estimated using single crystals is 9 K below that of the powder sample,[8] which also suggests that the physical properties of the compound are dependent on the samples.

NaV_2O_4 was recently discovered by Yamaura *et al.*[10] and Hirai *et al.*[11] independently, to join as a new member of this attractive family of calcium-ferrite-type vanadium oxides. Metallic conductivity along the b direction was clearly observed over the whole temperature range between 40 mK and 300 K using a single crystal, and a sharp antiferromagnetic transition was seen in the temperature dependence of the magnetic susceptibility at $T_N = 140$ K, above which a large Curie-Weiss behavior appeared. Each double chain is expected to be ferromagnetic and the chains order antiferromagnetically. Magnetic moments were reported to be collinear with the b direction, based on a large anisotropic drop of the susceptibility measured under 5 T. Thus, NaV_2O_4 presents a striking contrast to CaV_2O_4 from both electrical and magnetic viewpoints. Investigating changes in the physical properties of a solid-solution system of these two materials is the main aim of this study.

II. EXPERIMENT

Powder samples of $Ca_{1-x}Na_xV_2O_4$ ($0 < x \leq 1$) were synthesized using a belt-type high-pressure apparatus from stoichiometric mixtures of CaO, $Na_4V_2O_7$, and V_2O_3 sealed in Au capsules at 1300 °C for an hour under 6 GPa pressure. The sample was thermally quenched to room temperature and the pressure was then gradually reduced. CaO was previously obtained by decomposition of $CaCO_3$ at 1050 °C under flowing Ar gas. $Na_4V_2O_7$ was prepared from a stoichi-
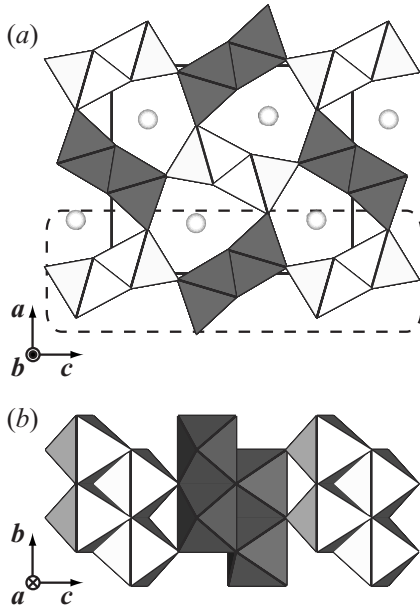
FIG. 1. Structure of AV_2O_4 (A=Ca,Na). The octahedra and the circles represent VO_6 octahedra and A ions, respectively. V ions in the dark octahedra are different from those in the light ones from the crystallographic viewpoint. The lattice axes are labeled based on the space group *Pnma* according to the previous report (Ref. 10). The square in panel *a* shows the unit cell, and panel *b* shows a part of the structure within the broken lines in panel *a* from a different angle.

ometric mixture of Na_2CO_3 and V_2O_5 in air at 550 °C with intermediate grindings. Since these precursors easily react with water and/or carbon dioxide in air, weighing, mixing and sealing of the compounds were performed in a dry box filled with Ar gas. CaV_2O_4 was made by flowing H_2/Ar gas at ambient pressure at 1000 °C for 6 h from CaV_2O_6, which was previously made from $CaCO_3$ and V_2O_5 at 700 °C in air. Since the CaV_2O_4 sample obtained was very fragile, CaV_2O_4 was heated at 1300 °C under 6 GPa pressure to obtain hard pellets for electrical resistivity and specific-heat measurements. Needlelike single crystals of NaV_2O_4 a few mm in length were grown from the mixture sealed in a Pt capsule with approximately 1 wt % water, which was gradually cooled down from 1600 to 800 °C under 6 GPa pressure. However, the growth was unsuccessful under synthetic conditions when a dry mixture with 0.5–30 mol NaCl for 1 mol NaV_2O_4 was used. The crystals obtained were dried in vacuum. No impurity phase was detected in the powder of the crushed crystals and magnetic susceptibility measured using many crystals quantitatively agreed with that of the powder sample. On the other hand, CaV_2O_4 single crystals failed to be grown from a mixture of $Ca(OH)_2$ and V_2O_3 under the pressure.

The sample quality was checked by powder x-ray diffraction (XRD) measurements performed on a commercial diffractometer (X'pert, Panalatica) using Cu K_α radiation. For $0.17 \leq x \leq 0.67$, a small amount of the secondary phase was detected, however, all the other samples were proved to be pure. Lattice constants estimated from the XRD patterns are shown in Fig. 2, and they were found to decrease with in-
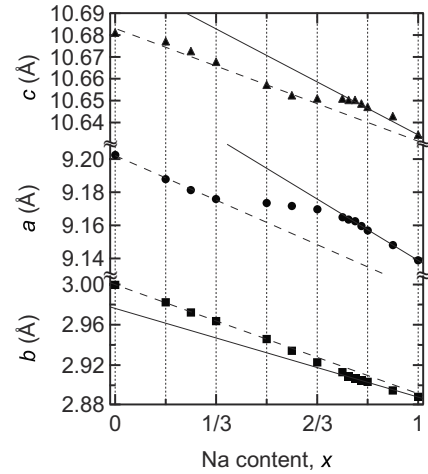

FIG. 2. Lattice constants of $Ca_{1-x}Na_xV_2O_4$. The solid lines are $a=9.250-0.1112x$, $b=2.976-0.0879x$, and $c=10.707-0.0727x$, while the broken lines are $a=9.202-0.0806x$, $b=3.000-0.1081x$, and $c=10.683-0.0516x$.

creasing x, which indicates the successful formation of a solid solution, and the b direction is influenced most by the substitution. The magnetization, M, was measured in the temperature range between $T=2-350$ K under various mag-
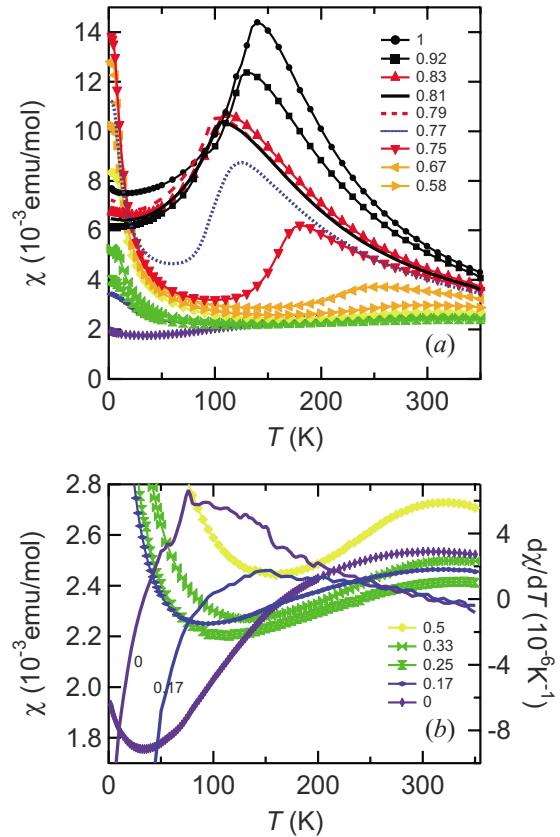

FIG. 3. (Color online) Magnetic susceptibility of $Ca_{1-x}Na_xV_2O_4$ with various x values measured under 1 T. The panel b magnifies the susceptibilities for $x \leq 0.5$ and shows the derivatives for $x=0$ (violet line) and 0.17 (blue line). The circle and square symbols in panel a are placed on every two points.
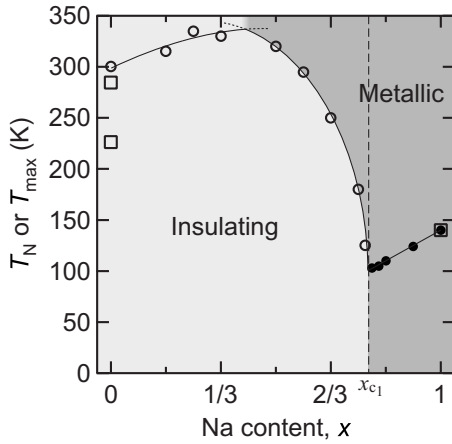
FIG. 4. Na content dependence of T_N and T_{max}. The full and open circles represent T_N and T_{max}, respectively, and the squares show T_N and T_{max} reported in Refs. 7, 8, and 10. The lines are included as guides for the eye. The metallic and insulating regions are colored dark and light, respectively.

netic fields of $H=0.001-7$ T using a commercial magnetometer with a superconducting quantum interference device produced by Quantum Design. In this paper, the magnetic susceptibility is simply defined to be $\chi=M/H$. The T_N value for $x>0.78$ was determined to be the temperature corresponding to the peak of the susceptibility. The electrical resistivity, ρ, and specific heat, C_p, were measured in the ranges of $T=2-400$ K and $H=0$ T for ρ, and $T=2-300$ K and $H=0-9$ T for C_p using the physical properties measurement system by Quantum Design.

III. RESULTS

A. Magnetism

Three parameters, x, T, and H, were tuned to study the magnetic properties of $Ca_{1-x}Na_xV_2O_4$. The temperature dependence of the magnetic susceptibility under 1 T is shown in Fig. 3. The susceptibilities for $x=0$ and 1 agree well with the values in previous reports.[7,8,10] The transition temperature T_N decreases with decreasing x down to $x=0.79$. For $x \leq 0.77$, the peak of the susceptibility becomes broader and the peak position, T_{max}, increases very rapidly. From $x \sim 0.33$ to $x=0$, T_{max} slightly decreases. These changes are summarized in Fig. 4. T_N decreases in accordance with the line of $T_N=-40.0+180x$, and below $x_{c_1} \sim 0.78$, it abruptly disappears and is replaced by T_{max}. The change from T_N to T_{max} is abrupt as the difference in the x values corresponds to only 0.01 for the vanadium formal valence.

Next, field effects on the magnetism of NaV_2O_4 are presented. Figure 5 shows magnetic susceptibilities under various magnetic fields and their derivatives. For the 1 T susceptibility, there is a bump around 126–130 K, and two characteristic temperatures can be defined; one is the bending point at $T_{n_1}=130$ K, below which the susceptibility deviates from that under 0.01 T, and the other is the kink at $T_{n_2}=126$ K, which almost corresponds to the peak in the derivative. As seen in Fig. 5, the former increases with increasing
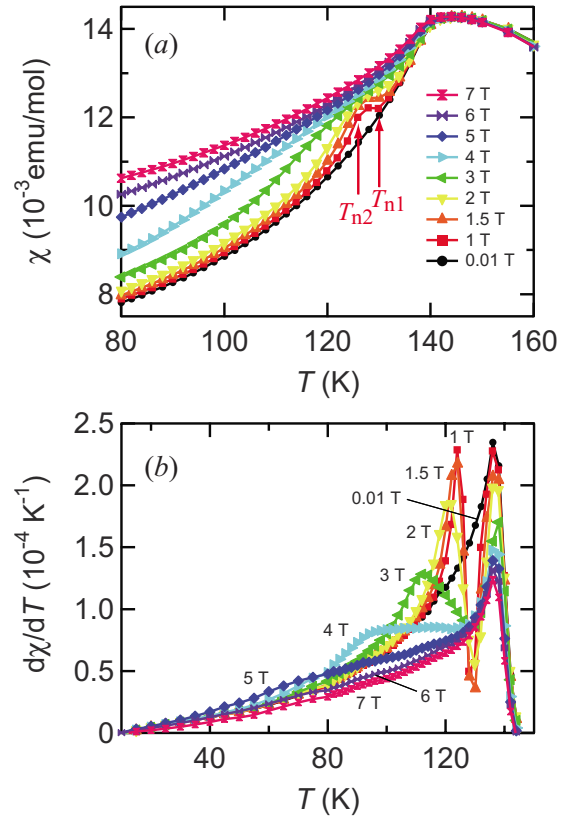

FIG. 5. (Color online) Magnetic susceptibilities of NaV_2O_4 ($x=1$) under various fields (a), and their derivatives (b).

field, while the latter decreases. No thermal hysteresis of T_{n_1} and T_{n_2} was detected. Some anomalies are also seen in the magnetization curves, as shown in Fig. 6; each magnetization curve below T_N bends at a certain field, H_c, as clearly seen in Figs. 6(c) and 6(d). The peak in the derivative of the magnetization curve moves to a lower field with increasing temperature up to 125 K, and then moves to a higher field. No field hysteresis was detected. Thus, the $H-T$ phase diagram may be drawn as indicated in Fig. 7. The antiferromagnetically ordered phase is divided into three regions of AF1, AF2, and AF3. It was hard to determine the existence of the AF2 phase in the absence of a field by these measurements; the kink in the susceptibility gradually became prominent with increasing field, and the slopes of the phase boundaries between AF1 and AF2, and between AF2 and AF3, are very large and small, respectively, below 0.5 T, which makes it impossible to estimate H_c by the isothermal magnetization curves.

The $H-T$ phase diagrams for $x=0.92$ and 0.83 are shown in Figs. 8 and 9, respectively. These were obtained in the same manner as in the case of $x=1$ from the magnetic data shown in Figs. 10–13. Interestingly, the phase relation between AF1, AF2, and AF3 strongly depends on the Na content; the AF3 phase is very strongly suppressed by the substitution of Na ions for Ca ions, and instead the AF1 and AF2 phases cover larger areas. The AF2 region at 1 T for $x=0.92$ is wider than that for $x=1$, although its presence at zero field is still unclear because of the same reason as mentioned above. Finally, AF3 disappears and the AF1 phase
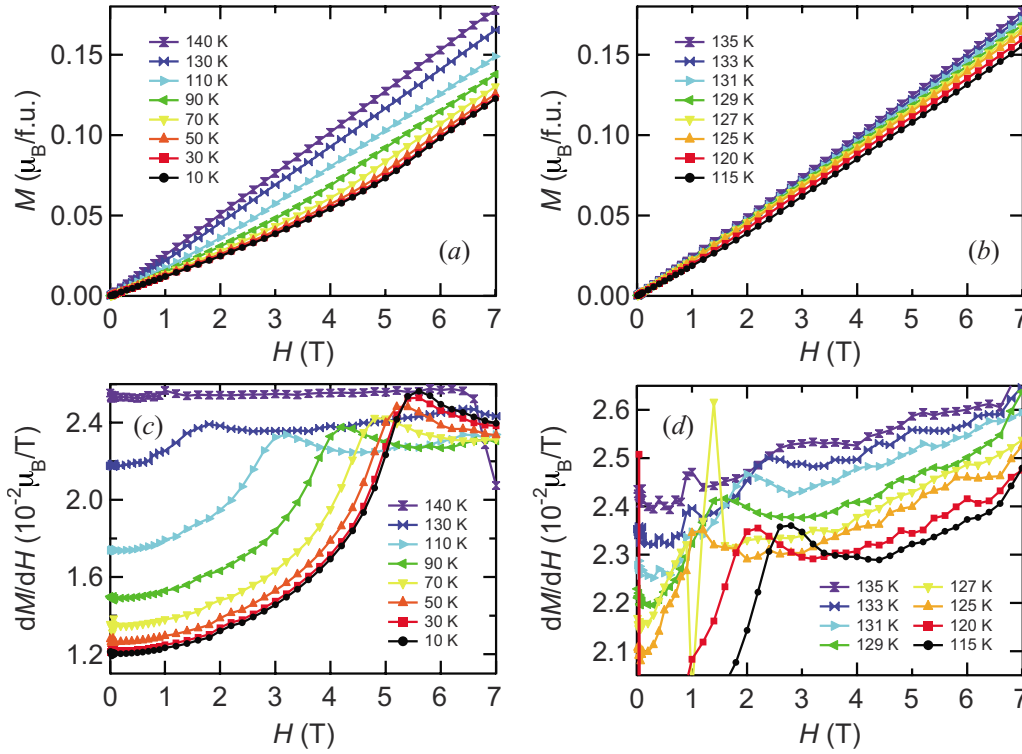
FIG. 6. (Color online) Magnetization curves of NaV_2O_4 at various temperatures (a, b), and their derivatives (c, d).

covers most of the low-field region below T_N. The phase boundary between AF1 and AF2 cannot be determined unambiguously for a low-field region, because the difference between T_{n_1} and H_c becomes larger. The field at which the derivative of the magnetization curve starts to increase may be more suitable for the position of H_c on the boundary. For $x=0.81$, 0.79 or 0.77, the phase relation was qualitatively the same as that for $x=0.83$, although the H_c values at 2 K were approximately 0.5, 1.1, or 1.1 T higher, respectively, than that for $x=0.83$. The magnetism of the $x=0.77$ sample seems to be complex because $x=0.77$ is smaller than x_{c_1}. The x_{c_1} value may slightly decrease with increasing field. For x

$=0.75$, no bending behavior in the magnetization curves at 2, 10, 50, and 100 K was observed below 7 T, and no significant difference was detected above 20 K in the temperature dependence of the susceptibilities under various fields up to 7 T. The upturn in the susceptibility below 20 K was suppressed by the field as observed for many paramagnets.

As seen in Fig. 3, susceptibility data above T_N or $T_{\max}$ for $x \geq 0.75$ seem to obey the Curie-Weiss law, which is represented by $\chi = C/(T-\theta) + \chi_0$ (C: Curie constant, θ: Weiss temperature, and χ_0: constant term). These parameters estimated using the data between 250 and 350 K are shown in Table I. The Curie constant values are close to the theoretical value of 1.38 emu K/mol, calculated assuming the local moments caused by $S_1=1/2$ on tetravalent vanadium ions and $S_2=1$ on
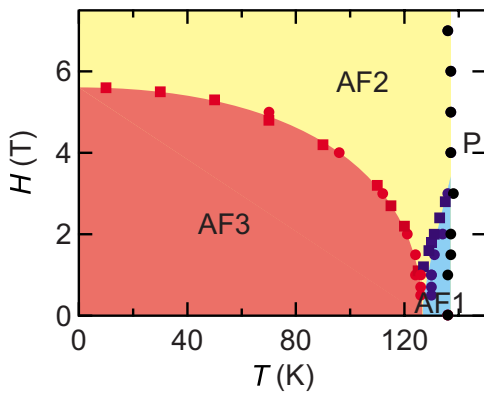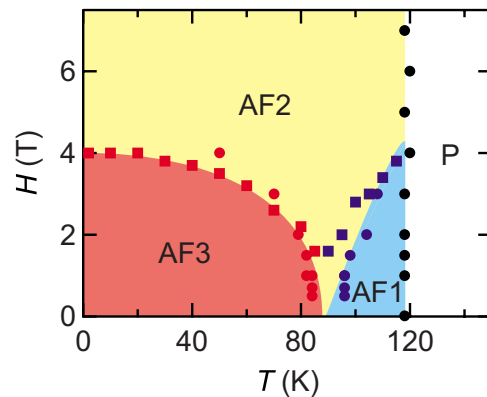

FIG. 7. (Color online) $H-T$ phase diagram for NaV_2O_4 ($x=1$). AF1, AF2, and AF3 represent three kinds of antiferromagnetic phases, while P represents the paramagnetic phase. The points marked by circles and squares were determined using the susceptibilities and magnetization curves, respectively. The colors are guides for the eye.

FIG. 8. (Color online) $H-T$ phase diagram for $Ca_{0.08}Na_{0.92}V_2O_4$ ($x=11/12$). The points marked by circles and squares were determined using the susceptibilities and magnetization curves, respectively. The colors are guides for the eye.

FIG. 9. (Color online) $H-T$ phase diagram for $Ca_{0.17}Na_{0.83}V_2O_4$ ($x=10/12$). The points marked by circles and squares were determined using the susceptibilities and magnetization curves, respectively. The colors are guides for the eye.
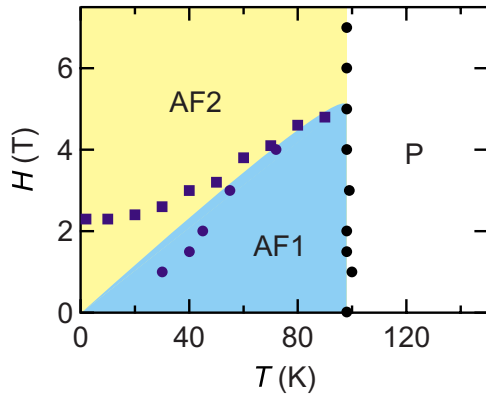
trivalent vanadium ions with a g-factor of 2. However, the x dependence of C, which seems to decrease with decreasing x, is inconsistent with the change in the valence under the local-moment assumption, because the number of trivalent vanadium ions with the larger spin increases with decreasing x. The Weiss temperature decreased with decreasing x and changed its signs at an x value between $x=0.75$ and 0.77, which is very close to x_{c_1}. The Curie-Weiss behavior at a high temperature range will be discussed later in detail.

A tiny anomaly was detected at 76 and 155 K in the susceptibility of CaV_2O_4, as shown in Fig. 3(b). The former agrees with T_N reported by Zong $et\ al.$[8] The magnetic ordering was undetectable above 76 K for $x=0.17$, and thus T_N for $x=0$ would not be on the line of $T_N=-40.0+180x$, which was estimated from T_N above x_{c_1}. Indeed, the line suggests that $T_N=0$ at $x=2/9=0.22$. On the other hand, the anomaly at 155 K probably corresponds to that seen at around 140 K of the specific heat, although the origin of this is unclear. Structural analysis should be carefully performed because the magnetic state will be strongly influenced by the structural transition, if it exists, due to spin frustrations on the double chains.

For $x<x_{c_1}$, large upturns are seen in the low-temperature regions. The upturn of CaV_2O_4 is extrinsic due to crystal
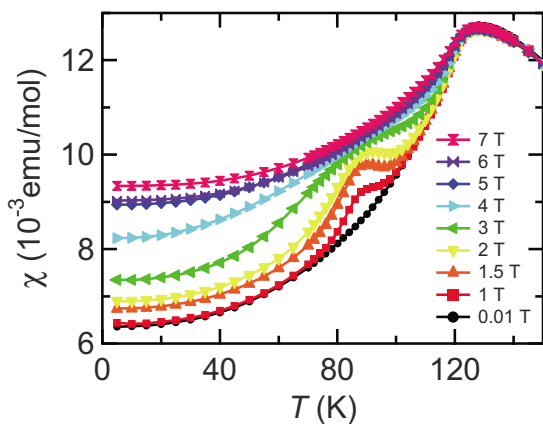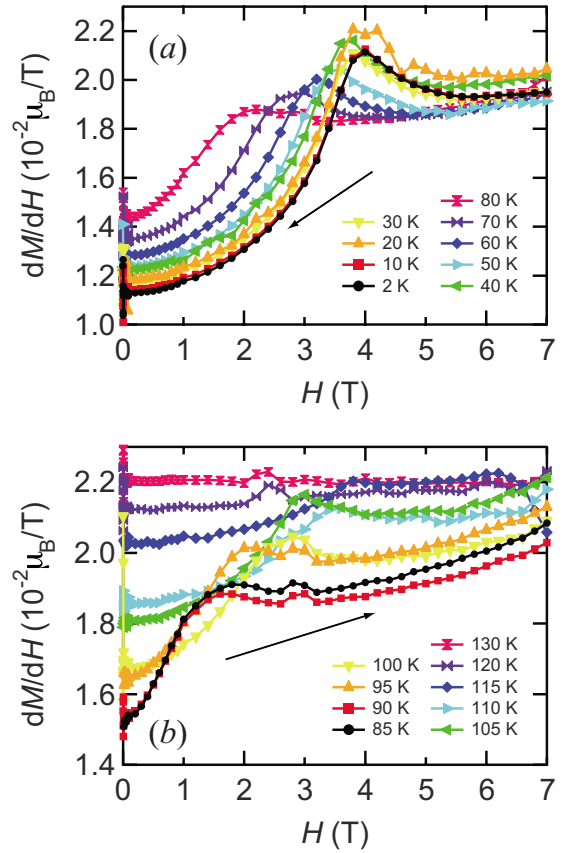

FIG. 11. (Color online) Derivatives of magnetization curves of $Ca_{0.08}Na_{0.92}V_2O_4$ ($x=11/12$) below 80 K (a) and above 85 K (b).

defects and/or undetectable magnetic impurities, because the compound shows the magnetic ordering at T_N. However, a part of each upturn for $x\neq0$ can be intrinsic because it increases significantly as shown in Table II. The Curie constant appears to increase according to $C=0.156x$, whose slope is 42% of that calculated assuming that one-Na ion substitution just makes one magnetic moment with $S=1/2$ and $g=2$ without any other change. On the other hand, spin-glass (SG) behavior was observed for $0.17\leq x\leq0.81$ below 16 K or lower. The SG transition temperature, T_{SG}, and the residual

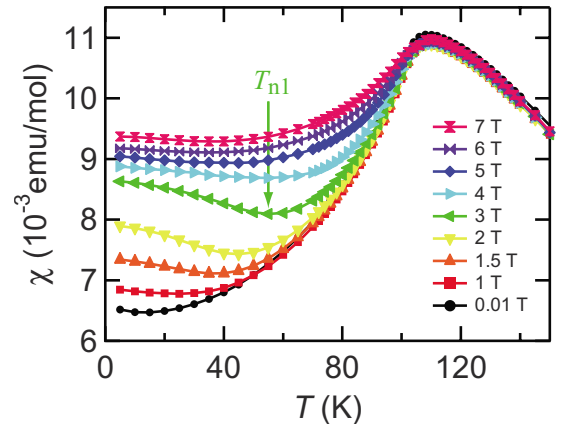
FIG. 10. (Color online) Magnetic susceptibilities of $Ca_{0.08}Na_{0.92}V_2O_4$ ($x=11/12$) under various fields.

FIG. 12. (Color online) Magnetic susceptibilities of $Ca_{0.17}Na_{0.83}V_2O_4$ ($x=10/12$) under various fields.

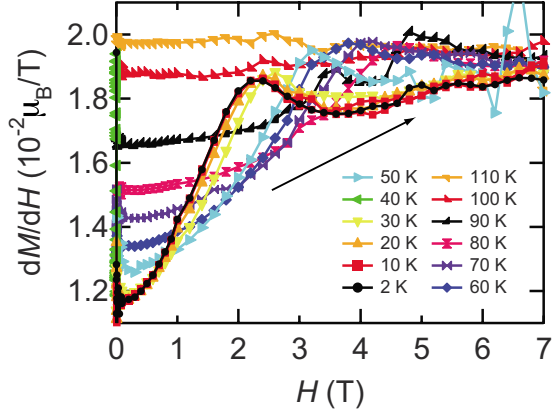FIG. 13. (Color online) Derivatives of magnetization curves of $Ca_{0.17}Na_{0.83}V_2O_4$ ($x=10/12$).

TABLE I. Parameters obtained by Curie-Weiss fit for the data between 250 and 350 K.

x	$12x$	C (emu K/mol)	θ (K)	χ_0 (10^{-4} emu/mol)
1	12	1.12	93.9	−0.738
0.92	11	1.29	63.7	−3.89
0.83	10	0.98	55.5	4.25
0.81	9.75	1.03	43.0	3.12
0.79	9.5	0.95	53.3	5.01
0.77	9.25	0.86	44.6	6.39
0.75	9	1.19	−17.1	3.72

magnetization, M_r, which was estimated using the data between 0.01 and 0.1 T by the linear function of $M=M_r+\chi H$, are summarized in Table II. This behavior can also be intrinsic because the x dependence of M_r corresponds well with that of the Weiss temperature. However, the following should be noted: (i) The CaV_2O_4 sample did not show SG behavior even under 0.001 T, although similar SG behavior was observed for a single crystal of CaV_2O_4,[8] and (ii) a kink was seen in zero-field cooling susceptibility under 0.001 T for $x=0.17$, 0.25, 0.33, and 0.5, around 5 K, independent of x. The latter implies that there is another SG component with $T_{SG}\sim5$ K probably due to the secondary phase, and that the SG behavior observed for $x\geq0.67$ is caused by this component.

B. Electrical resistivity

The temperature dependence of the electrical resistivity of $Ca_{1-x}Na_xV_2O_4$ ($x=0$, 0.17, 0.33, 0.5, 0.67, 0.75, 0.83, 0.92, and 1) is shown in Fig. 14. For $x\geq0.83$, the resistivities do not show a divergent behavior toward 0 K, which indicates metallic conductivity of these compounds. Indeed, single-crystal measurements proved metallic conductivity along the

b direction.[10] The negative temperature dependence is most likely due to grain-boundary scattering and/or possible semiconducting behavior along the a or c direction.

Metallic behavior was undetectable below 400 K for $x \leq 0.5$, while for $x=0.75$ and 0.67 in the middle x range, metal-insulator transitions (MIT) are clearly seen just around T_{max}. Since, from the band calculation, some kinds of the Fermi surface are expected to have a one-dimensional nature,[10,12] charge-density wave (CDW) or spin-density wave (SDW) formation can take place at T_{max}. The energy gap for $x\leq0.75$ is roughly estimated to be $\Delta\sim1000$ K from the data sufficiently below T_{max}. Assuming that the gap is caused by CDW/SDW formation, the CDW/SDW formation temperature may be calculated to be $T_c^{MF}=\Delta/(2\times1.76)\sim284$ K, based on the mean-field theory, which is comparable to T_{max}. As another possibility, charge ordering (CO) should also be taken into account, for comparison with vanadium hollandites.[1,3,4] $Bi_xV_8O_{16}$ shows MIT at $1.72<x<1.8$, wherein the V valence exactly corresponds to that of the $x=0.75$ or 0.67 compound. In addition, the MIT temperature of the Bi hollandites decreases with decreasing valence as in the present case. It should be noted that electrons in the CO state would be, in principle, bound to the V sites and can cause local moments, while spin degrees of freedom in the CDW state would almost disappear by Fermi degeneration.

TABLE II. Parameters obtained by Curie-Weiss fit to a low-temperature upturn, SG temperature, T_{SG}, and residual magnetization, M_r.

x	$12x$	C (10^{-2} emu K/mol)	$-\theta$ (K)	χ_0 (10^{-3} emu/mol)	T_{SG} (K)	M_r ($10^{-4}\mu_B$)
0	0	0.435	13.5	1.65	NA	0.101
0.17	2	2.20	0.95	1.92	16	3.49
0.25	3	2.86	1.52	1.85	14	4.45
0.33	4	4.29	2.50	1.82	10	8.63
0.5	6	9.09	5.33	1.66	6.5	9.09
0.58	7	9.82	4.31	1.66	5.5	6.63
0.67	8	11.0	3.41	1.63	5.0	5.42
0.75	9	10.5	2.16	1.75	4.8	5.33
0.77	9.25	5.65	0.13	3.47	4.8	3.55
0.79	9.5	NA	NA	NA	5.0	0.353
0.81	9.75	NA	NA	NA	5.0	0.0615

FIG. 15. (Color online) Temperature dependence of the specific heat of $Ca_{1-x}Na_xV_2O_4$ with various x values. The markers are placed on every two data points. Each curve, except that for $x=0$, is offset by 10 J/mol K interval to distinguish it from the others.

range ordering is seen in the susceptibility. Thus, local moments are considered to be absent. On the other hand, there is no anomaly around T_{n_1} and T_{n_2} as seen in Fig. 16(a), which suggests that changes in the magnetic states at these temperatures do not accompany changes in the entropy.

For $x=1$ and 0.83, the Sommerfeld constant and Debye temperature were estimated to be $\gamma=15.6$ mJ/mol K^2 and
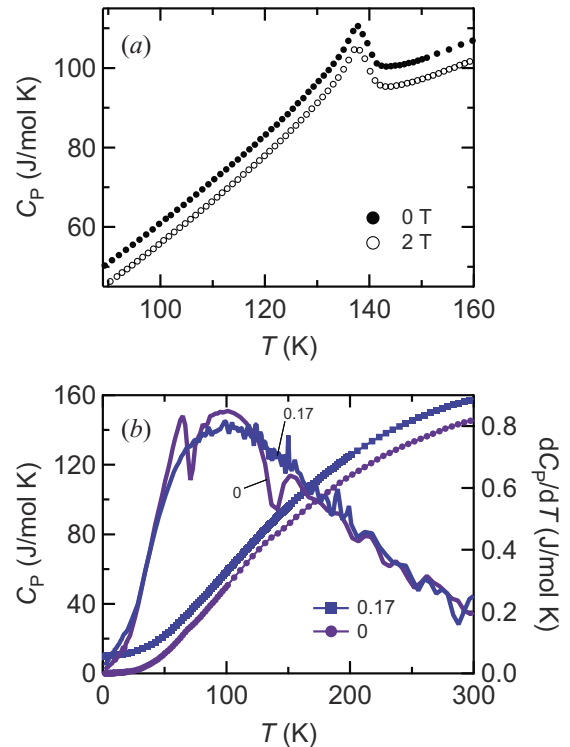
FIG. 16. (Color online) Temperature dependence of the specific heat of NaV_2O_4 (a) and CaV_2O_4 and $Ca_{0.83}Na_{0.17}V_2O_4$ and their derivatives (b). The 0 T curve in panel a and the $x=0.17$ curve in panel b are offset by 5 and 10 J/mol K, respectively.
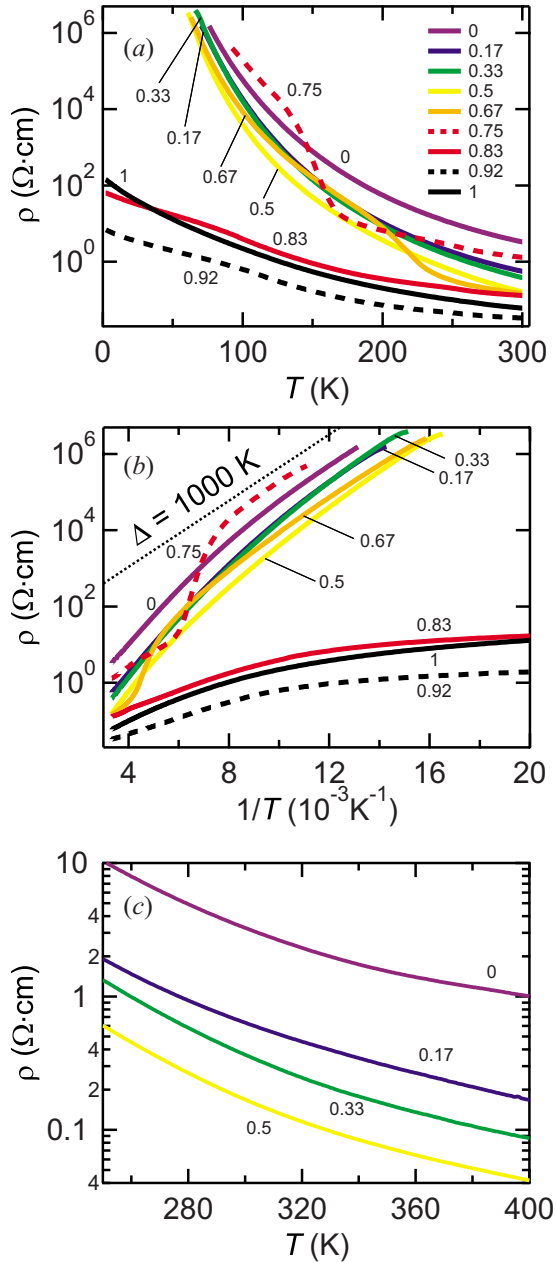

FIG. 14. (Color online) Temperature dependence of the electrical resistivity of $Ca_{1-x}Na_xV_2O_4$ with various x values (a,c) and the Arrhenius plot of the data in panel a (b). The dotted line in panel b shows the slope of $\Delta=1000$ K.

C. Specific heat

The temperature dependence of the specific heat for x $=0, 0.17, 0.33, 0.5, 0.67, 0.75, 0.83,$ and 1 are shown in Fig. 15. Sharp peaks are seen at T_N for $x=0.83$ and 1, and somewhat broad but clear anomalies can be recognized at T_{max}, at least for $x=0.75$ and 0.67. The entropy released at T_N was roughly estimated for NaV_2O_4 to be $S_e \sim 2$, which corresponds to the shadowed area in Fig. 15. This value is much smaller than the theoretical value of 14.9 $[=R \ln(2S_1 +1)(2S_2+2)]$ calculated assuming local moments on the vanadium ions. A significant part of the entropy cannot have been released above the transition since no sign of short-
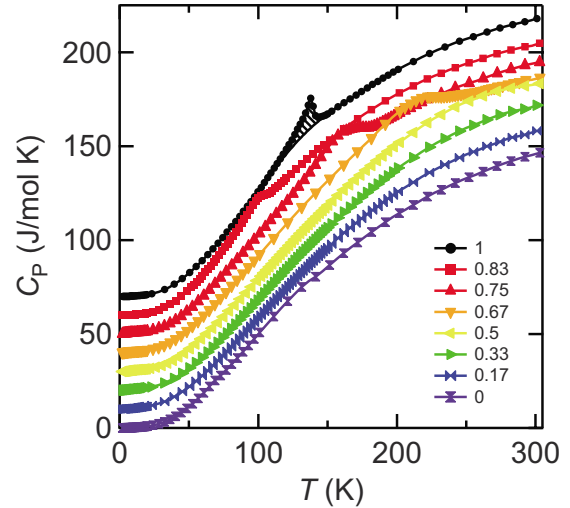
$\Theta = 576$ K, and $\gamma = 15.2$ mJ/mol K^2 and $\Theta = 516$ K, respectively, from the data below 20 K using the fitting function of $C_p/T = \gamma + AT^2 + BT^4$ [A and B: fitting parameters (A $\times 10^5$, B $\times 10^8$) = (7.14, 2.96) for $x = 1$, and (9.91, 1.89) for $x = 0.83$]. In the insulating region of $x \leq 0.75$, Schottky-type anomalies were seen just around 7–9 K as sometimes observed for insulating paramagnets. These are unlikely to be caused by the SG transition itself because the SG transition temperature depends more on the x value.

For CaV$_2$O$_4$, two tiny kinks were detected around 70 and 140 K, as seen in Fig. 16(b). The former is due to the antiferromagnetic ordering reported by Zong *et al.*,[8] while the latter probably corresponds to the small anomaly seen at 155 K in the susceptibility. However, these anomalies were not detected for $x \gtrsim 0.17$ at all. Thus, the antiferromagnetic state of CaV$_2$O$_4$ may not survive above $x = 0.17$.

IV. DISCUSSION

The physical properties of Ca$_{1-x}$Na$_x$V$_2$O$_4$ strongly depend on the Na content. For a higher x value above $x_{c_1} \sim 0.78$, the antiferromagnetic transition at T_N and metallic conductivity across the whole temperature range below 300 K were clearly observed. On the other hand, in the $x = 0.75$ or 0.67 samples, the MIT, probably due to the CDW/SDW formation or CO, occurs around T_{max}. This suggests a significant change in the band structure at x_{c_1}. On the other hand, it should be noted that another critical Na content, x_{c_2}, separates the phase below x_{c_1} into two regions; in the higher x region, the MIT takes place at T_{max}, while in the lower x region, the compound is electrically insulating below and above T_{max}. However, the x_{c_2} value cannot be determined exactly, because the MIT becomes less sharp with decreasing x. A value between 0.33 and 0.5 seems to be the most probable candidate; T_{max} decreases below the point and the x dependence of the lattice constants bend around the point, as seen in Fig. 2. Indeed, the specific heat for $x = 0.5$ appears to have a very broad anomaly around T_{max}, although no clear MIT was observed for this composition. Hereafter, the physical properties at each x range will be separately discussed in further detail, assuming that x_{c_2} is located between 0.33 and 0.5.

The first problem to be addressed concerns the existence or absence of local moments on vanadium ions above x_{c_1}. The Curie-Weiss behavior of magnetic susceptibility can appear either in the local-moment system or in an itinerant-electron system. However, for a typical itinerant-electron antiferromagnet, uniform susceptibility, namely the dynamical susceptibility at $\mathbf{q} = 0$, is not expected to show Curie-Weiss behavior although the dynamical susceptibility at $\mathbf{q} = \mathbf{Q}$ ($\mathbf{Q} \neq 0$: the antiferromagnetic wave vector) should show such a strong temperature dependence above T_N. Indeed, uniform susceptibility of V$_3$Se$_4$ is almost temperature independent above and even below T_N, but its NMR spin-lattice relaxation rate divided by the temperature, which is closely related to the most prominent component of the dynamical susceptibility, shows a strong temperature dependence.[13] Thus, NaV$_2$O$_4$ is not a typical antiferromagnetic metal.

Local moments may be defined on vanadium ions; only one electron on a vanadium ion may be localized and cause a local moment, and the rest of the 3d electrons (a half electron per vanadium ion for $x = 1$) can be delocalized acting as conducting electrons. A similar two-band mechanism has been proposed for spinel LiV$_2$O$_4$,[14] although the understanding of the electronic state of the spinel is still controversial. However, this idea seems less persuasive in the present case. The sharp change in the x dependence of T_N or T_{max} at x_{c_1} would not be expected for local-moment magnetism. The x dependence of the Curie constants shown in Table I and the small entropy change observed for $x = 1$ and 0.83 also seem to support the delocalization view. Furthermore, it should be noted that the magnetic properties of NaV$_2$O$_4$ are somewhat similar to those of V$_5$Se$_8$ and V$_5$S$_8$. These are metallic antiferromagnets without any local moments whose transition temperatures are $T_N = 27$ and 35 K, respectively.[13,15] Their magnetic susceptibilities show Curie-Weiss behavior with positive Weiss temperatures, and the ratios of T_N/θ for the two are 2.6 and 1.5, respectively,[13,15] which are comparable to $T_N/\theta = 1.5$ in the present case. For these compounds, two kinds of spin fluctuations have been proposed; one at $\mathbf{q} \neq 0$ causes magnetic ordering and the other at $\mathbf{q} = 0$ causes Curie-Weiss behavior of the uniform susceptibilities. This idea of a multi-$\mathbf{Q}$ state may be applicable to the present system although two facts should be taken into account: (i) Curie constants of the present system are close to the value of the local-moment system, which implies that spin fluctuations at $\mathbf{q} \neq 0$ would not be so strong that the antiferromagnetic fluctuations would overcome the ferromagnetic fluctuations, and (ii) T_N of the present system is independent of H below 7 T, which is in sharp contrast to the case of V$_5$Se$_8$.[13] One may think that electrons could be ferromagnetically itinerant only within the double chain. This idea might explain the magnetism discussed above. Indeed, ferromagnetic ordering has been theoretically expected on the railway trestle lattice of the double chain,[16] and NaV$_2$O$_4$ was proposed to have such a magnetic state although the proposal was based on a self-contradictory interpretation of the Curie-Weiss behavior and band structure.[10] However, this simple model of antiferromagnetically ordered ferromagnetic chains will never result in the existence of three magnetic phases of AF1–3 and the complex phase relationship between them. Indeed, preliminary data of neutron-scattering (NS) measurements refute the model. At present, it is unclear how the magnetic state of the present system is exactly described, however it is clear that local moments are not expected above x_{c_1}. Band calculations for the nonmagnetic state support this view, because they indicate that the electrons are highly itinerant.[10,12]

The antiferromagnetically ordered state of itinerant electrons, namely the SDW state, is brought about above x_{c_1}. Thus, a drop in the resistivity at T_N observed by single-crystal measurements should be discussed within the framework of SDW formation. Usually, SDW formation enhances the resistivity because the electron density decreases due to elimination of a part of the Fermi surface. Even in the case of a two-dimensional system, wherein a large part of the Fermi surface survives, the resistivity increases once just below T_N although the metallic state persists.[17] In the present case, the

metallic conductivity below T_N may result from the two-dimensional nature of the system, but the smooth decrease in the resistivity is very anomalous. First, of course, it would be necessary to clarify whether the drop is intrinsic, because the resistivity of the SDW system is generally very sensitive to the frequency of the measurement voltage.[18] If intrinsic, the situation is similar to that of Na_xCoO_2 ($x \sim 0.75$), as pointed out previously,[10] wherein the drop in the resistivity at the magnetic transition temperature is intuitively understood to be caused by ferromagnetic ordering in a CoO_2 layer, although the layers are antiferromagnetically ordered. However, there is no theoretical support for either compound. Moreover, the magnetic structure of NaV_2O_4 is not so simple, as discussed above. Thus, the mechanism of the resistivity drop must be reconsidered. It should be pointed out that large Curie-Weiss terms in the susceptibilities above the magnetic transition temperatures appear for both compounds in common. The Curie-Weiss behavior may be the key to understand the behavior of the resistivity.

Multiple subphases in an antiferromagnetic state have been observed in many SDW compounds.[19,20] The SDW state of the present system is divided probably by a change in the SDW wave vector as in other cases. It is hard to determine the wave vector in each phase from macroscopic experiments, however, the features of the AF1–3 phases can be shown; (1) the phase relation is very sensitive to x, T, and H, (2) T_N itself is independent of H despite 1, (3) the AF2 phase wedges itself between the AF1 and AF3 phases on the T−H phase diagrams, and (4) there is no significant change in the specific heat at the boundaries between them. Detailed band-structure calculations, as well as microscopic experiments including NS and NMR measurements, need to be performed.

For the insulating region below x_{c_2}, localized spins are expected, and the broad maximum in the susceptibility would be due to short-range ordering induced by possible spin frustrations and/or low-dimensional spin correlations in the double chains. However, no long-range antiferromagnetic ordering was detected above 2 K for $x \geq 0.17$. Gapless chiral order could be realized in this x region. The contradiction with regard to the magnetic order between the previous reports,[7,8] as well as the difference between the T_N values of the powder and crystal[8] and the SG behavior in a single crystal[8] may be due to a possible calcium deficiency.

Finally, the electronic state between x_{c_1} and x_{c_2} will be discussed. CDW/SDW formation or CO likely happens at T_{max} in this x range. If the former is the case, strong competition between the magnetic ordering at a higher x value and CDW/SDW formation at a lower x value may be inherent in this system. The MIT indicates that the electronic structure between x_{c_1} and x_{c_2} can be more perfectly one dimensional than the structure above x_{c_1}. This may be because the interchain distance becomes longer, as expected from the changes in the lattice constants. However, since the changes seem too small, some kinds of Fermi surface with a two- or three-dimensional nature can be reduced in size or could disappear completely by the substitution of Ca for Na. On the other hand, the large upturn in the susceptibility for $0.17 \leq x < x_{c_1}$ in a low-temperature region apparently seems to support CO,

because it can cause local moments below the MIT temperature, T_{MIT}. In this case, x_{c_2} may be just a crossover point where T_{MIT} becomes smaller than the original T_{max}. However, it is not obvious why susceptibility below x_{c_1} appears to be reproducible simply by superposition of the Curie-Weiss behavior on the susceptibility of CaV_2O_4 because one-Na ion substitution eliminates a trivalent vanadium ion with a larger spin, and yields a tetravalent ion. Although such a superposition has been observed when the original states are spin-singlet states,[21–24] in the present case all the magnetic moments should interact with each other at once and the susceptibility would need to be more significantly changed by the Na substitution.

In this section, the rich physical properties of the solid-solution system between NaV_2O_4 and CaV_2O_4 were discussed. The detailed measurements established the magnetic and electrical phase diagram of $Ca_{1-x}Na_xV_2O_4$ with three variables, x, T, and H. Further studies, such as NS, NMR, μSR, and electron spin resonance (ESR) measurements, are indispensable to determine the exact electronic state at each composition. This study will furnish a guide for such microscopic experiments and a basis to interpret the results obtained.

V. SUMMARY

The magnetic, electrical, and thermal properties of $Ca_{1-x}Na_xV_2O_4$ were investigated using samples with various x values ranging from 0 to 1 under various conditions of the temperature and magnetic field, to determine the x−T−H phase diagram. It was proved that the electronic state changes drastically at two critical compositions, x_{c_1} and x_{c_2}. Above an x_{c_1} of ~0.78, the antiferromagnetic state of the itinerant electrons is realized and T_N decreases from 140 to ~100 K with decreasing x. The antiferromagnetic phase was discovered to have three kinds of subphases, AF1, AF2 and AF3, depending sensitively on x, T, and H, above 2 K and below 7 T. AF1 is stable at a higher temperature and at a lower x value under a lower field, while AF3 is stable at a lower temperature and at a higher x value. The AF2 region extends widely under a higher field. This phase relation suggests the presence of the SDW state with a complex wave vector in each subphase. The Curie-Weiss behavior of the susceptibility above T_N was discussed. On the other hand, the x dependence of T_{max} and lattice constants suggests that x_{c_2} is located between 0.33 and 0.5, although the exact value was not determined. Below x_{c_2}, the compound is electrically insulating and localized spins are expected. The anomalies in the susceptibility and the specific heat due to the antiferromagnetic transition were confirmed for $x=0$, which agrees with a recent report.[8] However, no anomaly was detected for $x \geq 0.17$ above 2 K, suggesting that the antiferromagnetic state is stable only in the vicinity of $x=0$. Finally, the temperature-induced metal-insulator transition was, for the first time, observed at T_{max} between x_{c_1} and x_{c_2}. CDW/SDW formation and charge ordering were discussed as possible origins of the transition. This study revealed a variety of physical properties in the double chain and will stimulate further investigations.

ACKNOWLEDGMENTS

*sakurai.hiroya@nims.go.jp

[1] H. Kato, T. Waki, M. Kato, K. Yoshimura, and K. Kosuge, J. Phys. Soc. Jpn. **70**, 325 (2001).

[2] T. Waki, Y. Morimoto, H. Kato, M. Kato, and K. Kosuge, Physica B (Amsterdam) **329-333**, 938 (2003).

[3] T. Waki, H. Kato, M. Kato, and K. Yoshimura, J. Phys. Soc. Jpn. **73**, 275 (2004).

[4] M. Isobe, S. Koishi, N. Kouno, J. Yamaura, T. Yamauchi, H. Ueda, H. Gotou, T. Yagi, and Y. Ueda, J. Phys. Soc. Jpn. **75**, 073801 (2006).

[5] A. F. Reid, A. D. Wadley, and M. J. Sienko, Inorg. Chem. **7**, 112 (1968).

[6] K. Friese, Y. Kanke, A. N. Fitch, and A. Grzechnik, Chem. Mater. **19**, 4882 (2007), and references therein.

[7] H. Fukushima, H. Kikuchi, M. Chiba, Y. Fujii, Y. Yamamoto, and H. Hori, Prog. Theor. Phys. Suppl. **145**, 72 (2002).

[8] X. Zong, B. J. Suh, A. Niazi, J. Q. Yan, D. L. Schlagel, T. A. Lograsso, and D. C. Johnston, Phys. Rev. B **77**, 014412 (2008).

[9] J. M. Hastings, L. M. Corliss, W. Kunnmann, and S. La Placa, J. Phys. Chem. Solids **28**, 1089 (1967).

[10] K. Yamaura, M. Arai, A. Sato, A. B. Karki, D. P. Young, R. Movshovich, S. Okamoto, D. Mandrus, and E. Takayama-Muromachi, Phys. Rev. Lett. **99**, 196601 (2007).

[11] D. Hirai, T. Takayama, A. Yamamoto, D. Hashizume, and H. Takagi, Presentation in Spring Meeting of the Physical Society of Japan, 2007 (unpublished).

[12] M. Arai (private communication).

[13] Y. Kitaoka and H. Yasuoka, J. Phys. Soc. Jpn. **48**, 1460 (1980), and references therein.

[14] V. I. Anisimov, M. A. Korotin, M. Zolfl, T. Pruschke, K. LeHur, and T. M. Rice, Phys. Rev. Lett. **83**, 364 (1999).

[15] Y. Kitaoka and H. Yasuoka, J. Phys. Soc. Jpn. **48**, 1949 (1980), and references therein.

[16] S. Daul and R. M. Noack, Phys. Rev. B **58**, 2635 (1998).

[17] For example, N. P. Ong and J. W. Brill, Phys. Rev. B **18**, 5265 (1978).

[18] S. Donovan, Y. Kim, L. Degiorgi, M. Dressel, G. Grüner, and W. Wonneberger, Phys. Rev. B **49**, 3363 (1994).

[19] W. Kang, S. T. Hannahs, and P. M. Chaikin, Phys. Rev. Lett. **70**, 3091 (1993).

[20] S. A. Werner, A. Arrott, and H. Kendrick, Phys. Rev. **155**, 528 (1967).

[21] M. Hase, I. Terasaki, Y. Sasago, K. Uchinokura, and H. Obara, Phys. Rev. Lett. **71**, 4059 (1993).

[22] Y. Ajiro, T. Asano, F. Masui, M. Mekata, H. Aruga-Katori, T. Goto, and H. Kikuchi, Phys. Rev. B **51**, 9399 (1995).

[23] M. Azuma, Y. Fujishiro, M. Takano, M. Nohara, and H. Takagi, Phys. Rev. B **55**, R8658 (1997).

[24] Y. Uchiyama, Y. Sasago, I. Tsukada, K. Uchinokura, A. Zheludev, T. Hayashi, N. Miura, and P. Böni, Phys. Rev. Lett. **83**, 632 (1999).